Short Papers

Effect of Reflection on Gyrotron Operation

Edith Borie

***Abstract*—The effect of wave reflection on the single-mode operation of a gyrotron is investigated with the help of Rieke diagrams. For this purpose, a set of self-consistent equations describing the beam–field interaction is solved, taking into account the effect of the electron beam and the reflection coefficient on the frequency and RF field profile.**

***Index Terms*—Gyrotron, reflection.**

I. Introduction

The subject of the influence of reflections on gyrotron operation has been studied both theoretically [1]–[5] and experimentally [6], [7], [8], [9]. If the thickness of the output window has been matched to the operating wavelength, a nonzero reflection of parasitic modes can influence the operation of a gyrotron. This has been observed, for example, in [10]. In long pulse operation, the frequency varies with time. This has an effect on the efficiency and also influences the reflection coefficient. In this paper, we consider some effects of window reflection on single-mode operation of a gyrotron. For this purpose, a set of self-consistent equations describing the beam–field interaction is solved, taking into account the effect of the electron beam and the reflection coefficient on the frequency and RF field profile.

The amplitude of the reflection coefficient due to a ceramic window is easily computed [11]. The phase is affected by long-line effects [1], [6] and is generally very poorly known since it is difficult to measure. Even when long-line effects are relatively unimportant, as is the case when a built-in quasi-optical convertor is used, the phase of the reflection coefficient may be important. The influence of the phase of the reflection coefficient on the calculated output power and RF field profile is considered in this paper.

In many of the more recent theoretical papers, the time evolution of the amplitude was studied, but the longitudinal structure of the RF field profile was fixed. However, this is not always a good approximation, even for a matched load. This note reports on results calculated for the case that the longitudinal structure is not fixed.

After reviewing the basic equations, we present numerical results corresponding to experiments performed at the Forschungszentrum Karlsruhe (FZK), Eggenstein-Leopoldshafen, Germany, on frequency step tuning of a gyrotron designed to operate at 140 GHz in the $\mathrm{TE}_{22,6}$ mode [7], [8], [9].

II. Basic Equations

The equations describing gyrotron operation at arbitrary harmonics have been well known for a long time [13]–[15]. A derivation for the conventions used here is given, for example, in [16]–[18]. Define

$$\vec{u} = \gamma\vec{v}/c \tag{1}$$

Manuscript received May 25, 2000; revised November 2, 2000.

The author is with the Institute für Hochleistungsimpuls-und Mikrowellentechnik, Forschungszentrum Karlsruhe, 76344 Eggenstein-Leopoldshafen, Germany.

Publisher Item Identifier S 0018-9480(01)05063-3.

and

$$P = iu_\perp e^{-i(\Lambda+\theta_e)} = u_{\perp 0}\tilde{P} \tag{2}$$

where Λ is the slowly varying part of the gyrophase. The equation of motion for the electrons in the field of a TE_{mp} mode can be reduced to

$$u_z \approx \text{constant} \tag{3}$$

$$\frac{d\tilde{P}}{dz} + i\frac{\omega}{v_{z0}}\frac{1}{s}\left(\frac{\gamma}{\gamma_0}-1+\delta\right)\tilde{P} = -i\frac{\omega}{v_{z0}}\frac{\gamma}{\gamma_0}F_{mp}\hat{f}_{mp}(z) \cdot \left(\frac{ick_{mp}u_{\perp 0}\tilde{P}^*}{2\Omega_0}\right)^{s-1}. \tag{4}$$

Here, $\hat{f}(z)$ is the normalized field profile, Ω_0 is the nonrelativistic cyclotron frequency, and the detuning parameter δ is defined (with $s = 1$ for the first harmonic) as

$$\delta = 1 - \frac{s\Omega_0}{\gamma_0\omega}. \tag{5}$$

Also,

$$F_{mp} = \frac{eV_{\max}}{2mc^2}\frac{C_{mp}G_{mp}}{u_{\perp 0}}\frac{ck_{mp}}{\omega}\frac{1}{(s-1)!} \tag{6}$$

is related to the similar quantity used by Russian researchers [25], [26] by

$$F_G = \left(\frac{s\beta_\perp^2}{2}\right)^{s-2}F_{mp} \tag{7}$$

and

$$C_{mp}G_{mp} = \pm\frac{J_{m\pm s}(k_{mp}R_e)}{J_m(x_{mp})\sqrt{\pi(x_{mp}^2-m^2)}}. \tag{8}$$

The output power in the TE_{mp} mode is given by the Poynting vector. One can show that [16]

$$P_{\text{out}} = V_{\max}^2\,\mathrm{Re}\left(\frac{1}{2i\mu_0\omega}\hat{f}_{mp}\frac{d\hat{f}_{mp}^*}{dz}\right) \tag{9}$$

evaluated at the resonator output. Also note that

$$\frac{ck_{mp}u_{\perp 0}}{2\Omega_0} \simeq \frac{s\beta_{\perp 0}}{2}.$$

In a self-consistent formulation, the field profile satisfies

$$\frac{d^2F_{mp}\hat{f}}{dz^2} + \left(\frac{\omega^2}{c^2}-k_{mp}^2(z)\right)F_{mp}\hat{f} = -\tilde{I}\left(\frac{-ick_{mp}u_{\perp 0}}{\Omega_0}\right)^{s-1}\left\langle\tilde{P}^s\right\rangle. \tag{10}$$

Here,

$$\tilde{I} = \frac{eZ_0I_b}{2mc^2}\left(\frac{C_{mp}k_{mp}G_{mp}}{(s-1)!}\right)^2\cdot\frac{1}{u_{z0}}$$

where I_b is the beam current, $Z_0 = \sqrt{\mu_0/\epsilon_0}$, and $k_{mp}(z) = x_{mp}/R(z)$. If these equations are rewritten in terms of the independent variable $\tilde{z} = \omega z/v_{z0}$, they become essentially independent of the mode.

TABLE I
BEAM PARAMETERS CALCULATED WITH BFCRAY

accelerating voltage (kV)	81.2	83.4	84.0
coil currents (A)	90.5/34.9	98.4/37.2	100.5/35.8
B_{res} (T)	5.50	6.02	6.09
beam energy (keV)	76.5	78.4	78.9
beam current (A)	46.6	46.6	47.6
beam radius (mm)	8.2-8.4	8.1-8.3	7.9-8.1
$< \beta_\perp >$	0.378	0.371	0.402
$< \alpha >$	1.20	1.11	1.36

TABLE II
FREQUENCY AS FUNCTION OF MAGNETIC FIELD AND BEAM RADIUS FOR COROTATING $\mathrm{TE}_{25,6}$ AND $\mathrm{TE}_{22,7}$ MODES

mode TE_{mp}	B (T)	R_e=7.9 mm	R_e =8.0 mm	R_e =8.1 mm
22,7	6.03	150.924	150.898	n.s.
	6.05	150.946	150.915	150.875
	6.07	150.961	150.930	150.895
	6.09	150.976	150.946	150.909
25,6	6.03	151.181	151.189	151.196
	6.05	151.195	151.205	151.211
	6.07	151.210	151.220	151.215
	6.09	151.235	151.235	151.240

The reflection coefficient is given by

$$R = \frac{d\hat{f}_{mp}/dz + ik_z\hat{f}_{mp}}{d\hat{f}_{mp}/dz - ik_z\hat{f}_{mp}} \tag{11}$$

where $k_z = \sqrt{\omega^2/c^2 - k_{mp}^2}$. Since the load is not always ideally matched, the applicable boundary condition at the cavity output is $R = R_1$ for a given R_1. As mentioned in the introduction, the phase of R_1 is difficult to determine, even when the amplitude is known. A diagram giving the real and imaginary parts of R along contours of constant frequency and/or output power is known as a Rieke diagram [12].

III. NUMERICAL RESULTS

Input to any code dealing with the beam–field interaction in a gyrotron cavity requires a knowledge of the beam properties (total current, beam energy, velocity ratio) and the magnetic field in the resonator. Table I shows beam properties calculated with the BFCRAY computer code [22] for typical values of the experimental parameters.

Frequency pulling can have an effect on the reflection coefficient, especially if the load is not well matched. Table II shows approximate values of the frequency calculated self-consistently (assuming $|R| = 0$) for the corotating $\mathrm{TE}_{25,6}$ and $\mathrm{TE}_{22,7}$ modes as a function of the applied magnetic field for three-beam radii, assuming a current of 46.6 A and beam energy of 78.9 keV. For the $\mathrm{TE}_{25,6}$ mode, the average value of $\langle\alpha\rangle$ was 1.11, and for the $\mathrm{TE}_{22,7}$ mode it was increased to 1.37. The beam coupling factor for the $\mathrm{TE}_{25,6}$ mode was nearly constant, and, as expected, the frequency pulling does not depend much on the beam radius, in contrast to the case of the $\mathrm{TE}_{22,7}$ mode.

In single-mode approximation, the $\mathrm{TE}_{25,6}$ and $\mathrm{TE}_{22,7}$ modes can both oscillate at the given beam parameters. In fact, both rotation directions are possible in the case of the $\mathrm{TE}_{22,7}$ mode. The stability of an oscillating mode against perturbation by a parasitic mode was investigated using the cold-cavity fixed-field approximation for the field profiles [19], [20]. For a beam radius of 8.1 mm, the $\mathrm{TE}_{22,7}-$ mode was unstable against competition by both the $\mathrm{TE}_{22,7}+$ and $\mathrm{TE}_{25,6}-$ moded, for magnetic fields between 6.03–6.09 T. At a beam radius of 7.9 mm or less, it was stable. However, either of the other modes could oscillate if it started first. (These calculations were performed assuming no reflections.)

TABLE III
EFFECT OF PHASE OF REFLECTION COEFFICIENT ON GYROTRON OUTPUT, WITH POWER REFLECTION OF 1.5%, BEAM ENERGY 78.9 keV, $I = 46.6$ A, $B = 6.03$ T, BEAM RADIUS 7.9 mm, AND TWO VALUES OF AVERAGE VELOCITY RATIO. RESULTS FOR THE CASE OF A MATCHED LOAD ARE ALSO GIVEN

ϕ (deg)	F (GHz)	Q	P (kW)	F (GHz)	Q	P (kW)
$TE_{22,7-}$	$\alpha = 1.36$			$\alpha = 1.11$		
30	150.913	1950	942	150.893	1820	942
90	150.924	2050	932	150.906	1840	969
150	150.937	1750	1045	150.915	1660	1933
210	150.943	1415	1080	150.901	1290	817
270	150.924	1330	1025	150.873	1255	809
330	150.908	1520	1025	150.881	1550	915
$\|R\|$=0	150.924	1550	1020	150.898	1550	890
$TE_{22,7+}$	$\alpha = 1.36$			$\alpha = 1.11$		
30	150.963	2780	514	150.929	2027	791
90	150.971	2940	512	150.938	2172	782
150	150.983	2560	579	150.951	1904	852
210	150.997	1875	733	150.960	1572	887
270	151.004	1560	765	150.945	1389	896
330	150.981	1920	628	150.928	1585	885
$\|R\|$=0	150.982	1970	667	150.943	1660	887
$TE_{25,6-}$	$\alpha = 1.36$			$\alpha = 1.11$		
30	151.195	1970	860	151.171	1820	995
90	151.202	2120	860	151.182	1870	1015
150	151.216	1900	930	151.195	1690	1030
210	151.230	1570	990	151.195	1410	1000
270	151.224	1375	1005	151.170	1295	980
330	151.200	1715	868	151.163	1510	1020
$\|R\|$=0	151.212	1690	925	151.181	1550	1015

In the power balance equation for two interacting modes, the quality factor plays an important role [23]. We now demonstrate for the modes of interest that the quality factor depends sensitively on the (unknown) phase of the reflection coefficient and, hence, that mode competition will also be influenced.

Table III shows the frequency, quality factor, and output power calculated self-consistently for the $\mathrm{TE}_{22,7}-$, $\mathrm{TE}_{22,7}+$, and $\mathrm{TE}_{25,6}-$ modes. The beam energy was 78.9 keV, current was 46.6 A, magnetic field was 6.03 T, and beam radius was 7.9 mm. Average values of $\langle\alpha\rangle \approx 1.11$ and 1.36 were considered. The amplitude of $|R|$ was fixed to correspond to power reflection of 1.5%, and the phase was varied. For comparison, results calculated for a matched load ($|R| = 0$) are also given. It is obvious that the frequency shift, output power, and quality factor of a single mode depends sensitively on the phase of the reflection coefficient. For some values, the quality factor of one of the three competing modes is so much enhanced with respect to the other that it might be favored. However, the stability of a working mode does not seem to be determined only by the quality factor [21], [23].

Fig. 1 shows RF-field profiles for the $\mathrm{TE}_{22,7}+$ mode with $\alpha = 1.11$ and all other parameters, as in the table. The three curves show the (unnormalized) field profiles $V_{\max} \cdot \hat{f}$ for the following three cases:

1) matched load;
2) 1.5% power reflection and $\phi = 90°$;
3) 1.5% power reflection and $\phi = 270°$.

It is obvious that the RF field profile depends sensitively on the phase of the reflection coefficient, even when this has a rather small absolute value (here, $|R| = 0.1225$).

The results of calculations are qualitatively similar when $|R|$ is doubled (6% power reflection) and are summarized in Table IV and Fig. 2 for the case of the $\mathrm{TE}_{25,6}-$ mode, with a beam radius of 8.1 mm, $B = 6.03$ T, and velocity ratio of 1.11. The quality factor varies by a factor more than two, depending on the phase of the reflection coefficient.

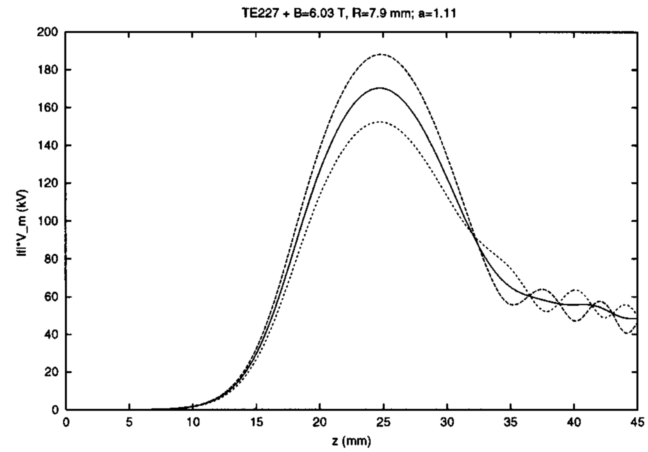

Fig. 1. RF field profiles $V_{\max} \cdot \hat{f}$ for the $\mathrm{TE}_{22,7}+$ mode for: matched load (solid curve), 1.5% power reflection and $\phi = 90°$ (long dashes), and 1.5% power reflection and $\phi = 270°$ (short dashes).

TABLE IV

EFFECT OF PHASE OF REFLECTION COEFFICIENT ON GYROTRON OUTPUT FOR THE COROTATING $\mathrm{TE}_{25,6}$ MODE, WITH POWER REFLECTION OF 6%, BEAM ENERGY OF 78.9 keV, $I = 46.6$ A, $B = 6.03$ T, BEAM RADIUS OF 8.1 mm AND AVERAGE VELOCITY RATIO OF $\alpha = 1.11$. RESULTS FOR THE CASE OF A MATCHED LOAD ARE ALSO GIVEN

ϕ (deg)	F (GHz)	Q	P (kW)
0	151.167	2029	881
90	151.189	2602	820
180	151.216	1750	1038
270	151.224	1238	893
$\lvert R\rvert$=0	151.196	1582	977

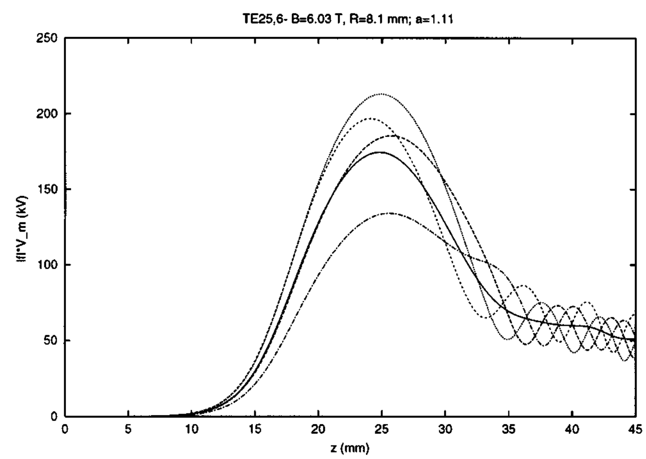

Fig. 2. RF field profiles $V_{\max} \cdot \hat{f}$ for the $\mathrm{TE}_{25,6}-$ mode for: matched load (solid curve), 6% power reflection and $\phi = 0°$ (long dashes), 6% power reflection and $\phi = 180°$ (short dashes), 6% power reflection and $\phi = 90°$ (dots), and 6% power reflection and $\phi = 270°$ (dashed–dotted).

Fig. 3 shows a Rieke diagram for the $\mathrm{TE}_{25,6}-$ mode corresponding to the parameters used in Table IV and Fig. 2. As also observed by other authors [6], there is a region where equifrequency lines converge and where two or more frequencies can be present simultaneously, for the same load characteristics. This "unstable region" occurs for $|R|$ slightly less than 0.4 and phase $\phi \approx 240°$. In most cases investigated numerically, this occurred for a phase of the reflection coefficient ϕ slightly less than 270°. This may explain why the field profile is so strongly distorted in this region. For other cases, the Rieke diagram provides other information [1].

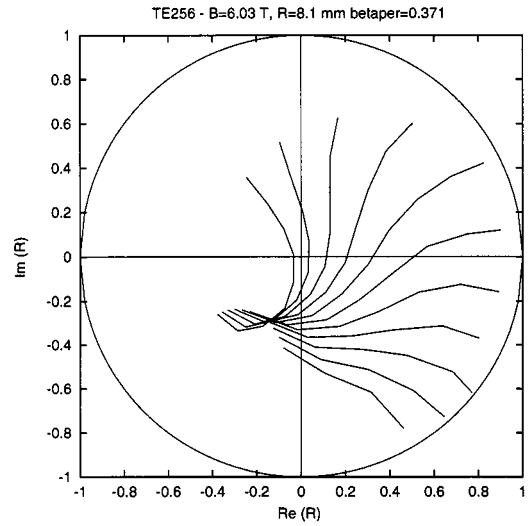

Fig. 3. Rieke diagram for the $\mathrm{TE}_{25,6}-$ mode with beam energy of 78.9 keV, $I = 46.6$ A, $B = 6.03$ T, beam radius of 8.1 mm, and average velocity ratio $\alpha = 1.11$. The equifrequency lines cover the frequency range 151.10–151.20 GHz in steps of 10 MHz.

IV. CONCLUSIONS

The effect of reflection on the behavior of a 1-MW 140-GHz gyrotron has been investigated for some experimentally relevant parameters. The effect of the electron beam and reflection coefficient on the frequency and RF field profile has been taken into account. The use of Rieke diagrams has been useful for this purpose. A quantitative fit to the data has not been performed. One may make the following qualitative conclusions.

- Power reflection back into the gyrotron cavity frequently has a significant effect on the RF field profile. Calculations using a fixed Gaussian field profile may not be as accurate as one might wish.
- The (poorly known) phase of the reflection coefficient is important, even in single-mode approximation. The field profile, output power, and quality factor depend sensitively on it, even for small values of $|R|$.
- Frequency pulling depends on the magnetic field, beam radius, velocity ratio, and reflection coefficient. Its magnitude varies from about 50 to 100 MHz, which is significantly less than the separation of the $\mathrm{TE}_{25,6}$ and $\mathrm{TE}_{22,7}$ modes in cold-cavity approximation (260 MHz).
- Long line effects basically change the phase and spread out the Rieke diagram.
- Mode competition calculations including the dependence on the phase of the reflection coefficient (which will be different for each mode), will be computationally very expensive; however, by not including it, it is unlikely to be sufficiently accurate.

ACKNOWLEDGMENT

The author would like to thank P.-K. Liu, Institute für Hochleistungsimpuls-und Mikrowellentechnik, Forschungszentrum Karlsruhe, Eggenstein-Leopoldshafen, Germany, J. Anderer, Institute für Hochleistungsimpuls-und Mikrowellentechnik, Forschungszentrum Karlsruhe, Eggenstein-Leopoldshafen, Germany, and M. Thumm, Institute für Hochleistungsimpuls-und Mikrowellentechnik, Forschungszentrum Karlsruhe, Eggenstein-Leopoldshafen, Germany, for a critical reading of this paper's manuscript and useful suggestions, and O. Braz, formerly of Institute für Hochleistungsimpuls-und Mikrowellentechnik, Forschungszentrum Karlsruhe, Eggenstein-Leopoldshafen, Germany, for stimulating discussions.

References

[1] E. Borie and B. Jödicke, "Rieke diagrams for gyrotrons," *Int. J. Infrared Millimeter Waves*, vol. 11, pp. 243–250, 1990.

[2] T. M. Antonsen, S. Y. Cai, and G. S. Nusinovich, "Effect of window reflection on gyrotron autooscillations," *Phys. Fluids*, vol. B4, pp. 4131–4139, 1992.

[3] M. Yu. Glyavin and V. E. Zapevalov, "The influence of reflections on the stability of gyrotron autooscillations," *Radiophys. Quantum Electron.*, vol. 41, pp. 916–922, 1998.

[4] ——, "Reflections influence on gyrotron oscillation regimes," *Int. J. Infrared Millim. Waves*, vol. 19, pp. 1499–1511, 1998.

[5] M. Yu. Glyavin, V. E. Zapevalov, and M. L. Kulygin, "Nonstationary processes in a gyrotron with reflections from output-section inhomogeneities," *Radiophys. Quantum Electron.*, vol. 41, pp. 1096–1100, 1998.

[6] P. Muggli, M. Q. Tran, T. M. Tran, H.-G. Mathews, G. Agosti, S. Alberti, and A. Perrenoud, "Effect of power reflection on the operation of a low-Q 8 GHz gyrotron," *IEEE Trans. Microwave Theory Tech.*, vol. 38, pp. 1345–1351, Sept. 1990.

[7] G. Dammertz, O. Braz, M. Kuntze, B. Piosczyk, and M. Thumm, "Influence of window reflections on gyrotron operation," in *22nd Int. Infrared Millimeter Waves Conf.*, H. P. Freund, Ed., 1997, paper T4.7, pp. 150–151.

[8] O. Braz, G. Dammertz, M. Kuntze, and M. Thumm, "D-band frequency step tuning of a 1 MW gyrotron using a Brewster output window," in *22nd Int. Infrared Millimeter Waves Conf.*, H. P. Freund, Ed., 1997, paper T4.5, pp. 147–149.

[9] G. Dammertz, O. Braz, A. K. Chopra, K. Koppenburg, M. Kuntze, B. Piosczyk, and M. Thumm, "Recent results of the 1-MW, 140-GHz, $\mathrm{TE}_{22,6}$-mode gyrotron," *IEEE Trans. Plasma Sci.*, vol. 27, pp. 330–339, Apr. 1999.

[10] G. Gantenbein, E. Borie, G. Dammertz, M. Kuntze, H.-U. Nickel, B. Piosczyk, and M. Thumm, "Experimental results and numerical simulations of a high power 140 GHz gyrotron," *IEEE Trans. Plasma Sci.*, vol. 22, pp. 861–870, Oct. 1994.

[11] H.-U. Nickel, "Hochfrequenztechnische aspekte zur entwicklung rückwirkungsarmer ausgangsfenster für millimeterwellengyrotrons hoher leistung," FZK, Eggenstein-Leopoldshafen, Germany, Sci. Rep. FZKA 5513, 1995.

[12] A. Frieser, *Mikrowellenmesstechnik*. Berlin, Germany: Springer-Verlag, 1965, sec. 4.4.

[13] V. L. Bratman, M. A. Moiseev, M. I. Petelin, and R. E. Erm, "Theory of gyrotrons with a non-fixed structure of the high frequency field," *Radio Phys. Quantum Electron.*, vol. 16, pp. 474–480, 1973.

[14] V. L. Bratman, M .A. Moiseev, and M. I. Petelin, *Gyrotrons: Collected Papers*. Gorki, Russia: USSR Acad. Sci., Inst. Appl. Phys., 1981.

[15] I. G. Zarnitsina and G. S. Nusinovich, "Competition between modes resonant with different harmonics of the cyclotron frequency in gyromonotrons," *Rad. Phys. Quantum Electron.*, vol. 20, pp. 461–467, 1977.

[16] E. Borie, *Gyrotron Oscillators—Their Principles and Practice*, C. J. Edgcombe, Ed. New York: Taylor & Francis, 1993, ch. 3.

[17] ——, "Self-consistent code for a 150 GHz gyrotron," *Int. J. Infrared Millim. Waves*, vol. 7, pp. 1863–1879, 1986.

[18] A. W. Fliflet, M. E. Read, K. R. Chu, and R. Seeley, "A self-consistent field theory for gyrotron oscillators: Application to a low Q gyromonotron," *Int. J. Electron.*, vol. 53, pp. 505–521, 1982.

[19] E. Borie and B. Jödicke, "Startup and mode competition in a 150 GHz gyrotron," *Int. J. Infrared Millim. Waves*, vol. 8, pp. 207–226, 1987.

[20] ——, "Self-consistent theory of mode competition for gyrotrons," *Int. J. Electron.*, vol. 72, pp. 721–744, 1992.

[21] E. Borie, G. Gantenbein, B. Jödicke, G. Dammertz, O. Dumbrajs, T. Geist, G. Hochschild, M. Kuntze, H.-U. Nickel, B. Piosczyk, and M. Thumm, "Mode competition using TE_{03} gytrotron cavities," *Int. J. Electron.*, vol. 72, pp. 687–720, 1992.

[22] E. Borie, C. Grüber, and T. Westermann, "Calculation of MIG guns for gyrotrons using the BFCPIC code," *Int. J. Electron.*, vol. 78, pp. 789–807, 1995.

[23] B. Jödicke, Forschungszentrum Karlsruhe, Eggenstein-Leopoldshafen, Germany, Sci. Rep. KfK 4603, 1989.

[24] E. Borie, *Gyrotron Oscillators—Their Principles and Practice*, C. J. Edgcombe, Ed. New York: Taylor and Francis, 1993.

[25] G. S. Nusinovich and R. E. Erm, "Elektron UHF" (in Russian), *Elektron. Tekh.*, ser. 1, vol. 8, p. 55, 1972.

[26] K. E. Kreischer, B. G. Danly, J. B. Schutkeker, and R. J. Temkin, "The design of megawatt cyrotrons," *IEEE Trans. Plasma Sci.*, vol. PS-13, pp. 364–373, Mar. 1985.

[27] G. Dammertz, O. Braz, C. T. Iatrou, M. Kuntze, A. Möbius, B. Piosczyk, and M. Thumm, "Long pulse operation fo a 0.5 MW $\mathrm{TE}_{10,4}$ gyrotron at 140 GHz," *IEEE Trans. Plasma Sci.*, vol. 24, pp. 570–578, May 1996.

An Efficient Krylov-Subspace-Based Algorithm to Solve the Dielectric-Waveguide Problem

Kaladhar Radhakrishnan and Weng Cho Chew

***Abstract*—An efficient scheme based on the bi-Lanczos algorithm has been developed for analysis of the dielectric-waveguide problem. A two-dimensional finite-difference scheme in the frequency domain is used to discretize the waveguide cross section. The resulting sparse eigenvalue problem is solved efficiently using the bi-Lanczos algorithm. Apart from solving the modes of the dielectric waveguide, a scheme to solve for the fields in the presence of a localized source is also described. Numerical results are also included to confirm the validity of the method.**

***Index Terms*—Bi-Lanczos algorithm, finite difference, optical waveguides.**

I. Introduction

In recent years, advances in optical waveguide technology have established the need for numerical algorithms to carry out the modal analysis for dielectric waveguides. Dielectric waveguides used in integrated optics consist primarily of rectangular dielectric cores. Since waveguides of rectangular cross section have no closed-form solution, the eigenmodes of the waveguide have to be found numerically. Several numerical methods are available to solve for the modes of dielectric waveguides. The dielectric waveguides were first analyzed using the mode-matching technique [1]. Goell [2] analyzed the same problem by expanding the field using circular harmonics. More recently, with the increase in the computational power of the computers, finite-element [3], [4] and finite-difference [5]–[8] techniques were used to solve the dielectric-waveguide problem. Schweig *et al.* [5] used the $E_z - H_z$ formulation to solve the problem. However, this formulation suffered from the occurrence of spurious modes. To avoid the spurious modes, Bierwirth *et al.* [6] used the transverse-field components to formulate the problem. This results in a sparse asymmetric matrix that is free of

Manuscript received June 1, 1998; revised August 28, 2000. This work was supported by the Multidisciplinary University Research Initiative Program under Grant F49620-96-1-0025, by the National Science Foundation under Electrical and Communications Systems Grant 93-02145, and by the Office of Naval Research under Grant N00014-95-1-0872.

K. Radhakrishnan was with the Center for Computational Electromagnetics, Department of Electrical and Computer Engineering, University of Illinois at Urbana-Champaign, Urbana, IL 61801 USA. He is now with the Intel Corporation, Chandler, AZ 85226 USA (e-mail: kaladhar.radhakrishnan@intel.com).

W. C. Chew is with the Center for Computational Electromagnetics, Department of Electrical and Computer Engineering, University of Illinois at Urbana-Champaign, Urbana, IL 61801 USA.

Publisher Item Identifier S 0018-9480(01)05054-2.